Glass-Fiber-Reinforced Polypropylene/EPDM Blend. I. Melt Rheological Properties

A. K. GUPTA, P. KRISHNA KUMAR, and B. K. RATNAM

Centre for Materials Science and Technology, Indian Institute of Technology, New Delhi-110016, India

SYNOPSIS

Melt rheological properties of the blend of isotactic polypropylene (PP) and ethylene propylene diene rubber (EPDM) at varying ratios and of the glass fiber (GF) filled PP and PP/EPDM blend by varying both GF loading and blending ratio of the polyblend matrix are studied. Rheological measurements at 220°C in shear rate range 10^1–10^4 s^{-1} were made on a capillary rheometer. Scanning electron micrographs of the extrudates are presented to show the morphology and the alignment of the glass fibers with respect to the flow direction. Variations of pseudoplasticity index, melt viscosity, and melt elasticity with EPDM content in PP/EPDM blend, and with varying GF content at any given composition of the matrix in PP/EPDM/GF ternary system, in the studied range are presented and discussed. Results on melt viscosity and melt elasticity show (i) reduced effect of GF at high shear rates on these properties and (ii) upward deviation of melt viscosity versus shear rate curve at low shear rates. A change in flow behavior in presence of GF is observed around a critical shear rate 2×10^3 s^{-1} and is attributed to the difference of interaction of GF and the dispersed rubber droplets at high and low shear rates. Elastic recovery showed nonequilibrium behavior at low shear rates.

INTRODUCTION

Rheological properties of polymer melts dictate the choice of processing conditions and influence the morphology and thereby the mechanical and physical properties of the finished product. Knowledge of such properties, particularly for multiphase polymeric fluids, which is of immense importance in view of the widespread use of polymer blends and composites, is still in its infancy. Among the multiphase systems, those involving mixtures of two or more polymers have attracted greater attention than the ones with rigid suspensions. The current status of knowledge for both these types of multiphase systems is presented by Han.[1]

Melt rheology of polymers in presence of rigid suspensions such as $CaCO_3$,[4,8,15,16] TiO_2,[2,8] carbon black,[3,5,8] carbon fibers,[15] talc,[10,14,15] glass beads,[4,10,17] and glass fibers[6,7,9,11–13,15] has been studied extensively. Effect of glass fiber (GF) on melt rheology of polyethylene,[7,15] polypropylene,[4,6,12,13,15] polystyrene,[7,9] polybutyleneterephthalate,[11] and nylon 66,[13] reported in literature, clearly justifies need for investigation on more systems for achieving better understanding of the processing parameters of GF-reinforced thermoplastics.

The present paper aims to add to the knowledge in this area through a study on GF filled polyblend of PP and the copolymer of ethylene propylene and diene monomer (EPDM elastomer). Data on unfilled PP/EPDM blend at varying blending ratios are also presented to serve as reference data for describing the effect of glass fiber in PP/EPDM/GF composite. Furthermore, these data on PP/EPDM binary blend cover a wide range of composition and experimental variables, and can thus be regarded as an additional system for the melt rheological studies of PP based blends reported from the authors' laboratory.[18–20] The data on PP/GF at varying GF content are presented to represent the case of 0% EPDM content of the PP/EPDM/GF composite.

Journal of Applied Polymer Science, Vol. 42, 2595-2611 (1991)
 CCC 0021-8995/91/092595-17$04.00

EXPERIMENTAL

Materials

Isotactic polypropylene (PP) of Indian Petrochemicals Corporation Ltd., molding grade "Koylene M 0030" of melt flow index 10.0, was used.

Elastomer EPDM used was a random copolymer, Nordel 1040 of DuPont. Ethylene and diene contents of the EPDM, determined by IR spectroscopy were 75 and 4%, respectively, and the Mooney viscosity of the copolymer was 40.

Glass fibers used were the chopped strands of lengths 3 mm and coated with a proprietary coupling agent suitable for use with polypropylene, supplied by Fibre-glass Pilkington Ltd. (commercial name: FGP-1651).

Preparation of Blends and Composites

PP/EPDM blends were prepared by melt blending in a single screw extruder (Windsor SX-30) at screw speed of 20 rpm and temperature range of 200–220°C from the first zone to the die.

The PP/EPDM/GF composites were prepared by mixing appropriate quantities of the three components in the extruder under the conditions similar to those described above for the case of the binary blend.

Nomenclature and the compositions of the various samples studied are shown in Table I. The compositions were so chosen that binary blend at three blending ratios (w/w), viz. 90/10, 80/20, and 70/30 and the unblended PP, were used as the matrix of the composites at three fixed GF contents (viz., 10, 20, and 30 wt %) in each composition of the matrix.

The thick strands received from the extruder were cut into small granules in a granulator, which were used for rheological measurements.

Measurements and Analysis Procedure

Melt rheological measurements were made on a piston type capillary rheometer (Goettfert Werkstoff Proefmaschinen Rheograph 2001, Version 9.6) having a circular die of L/D ratio 30. Measurements were made at a fixed temperature 220°C in the range of shear rate 10^1–10^4 s^{-1}.

Apparent shear rate ($\dot{\gamma}_{app}$) and shear stress ($\tau_{w/app}$ were calculated by the following relations[21]:

$$\dot{\gamma}_{app} = 4\dot{V}/\pi R^3$$

where R is the radius of the capillary die and $\dot{V}$ is the volumetric flow rate. True shear rate $\dot{\gamma}$ was determined by applying the Rabinowitsch correction[21]

$$(\tau_w)_{app} = \frac{P \cdot D}{4L}$$

where P is the pressure applied on the piston and L and D are length and diameter of the capillary. True

Table I Nomenclature and Composition of the Samples Studied

Sample Designation	Description	Composition (wt %)			
		PP	EPDM	PP/EPDM	GF
A	PP	100	—	—	—
E	EPDM	—	100	—	—
P1	PP/GF (90/10)	90	—	—	10
P2	PP/GF (80/20)	80	—	—	20
P3	PP/GF (70/30)	70	—	—	30
B1	PP/EPDM (90/10)	90	10	—	—
B2	PP/EPDM (80/20)	80	20	—	—
B3	PP/EPDM (70/30)	70	30	—	—
C1	B1/GF (90/10)	—	—	90	10
C2	B1/GF (80/20)	—	—	80	20
C3	B1/GF (70/30)	—	—	70	30
C4	B2/GF (90/10)	—	—	90	10
C5	B2/GF (80/20)	—	—	80	20
C6	B2/GF (70/30)	—	—	70	30
C7	B3/GF (90/10)	—	—	90	10
C8	B3/GF (80/20)	—	—	80	20
C9	B3/GF (70/30)	—	—	70	30

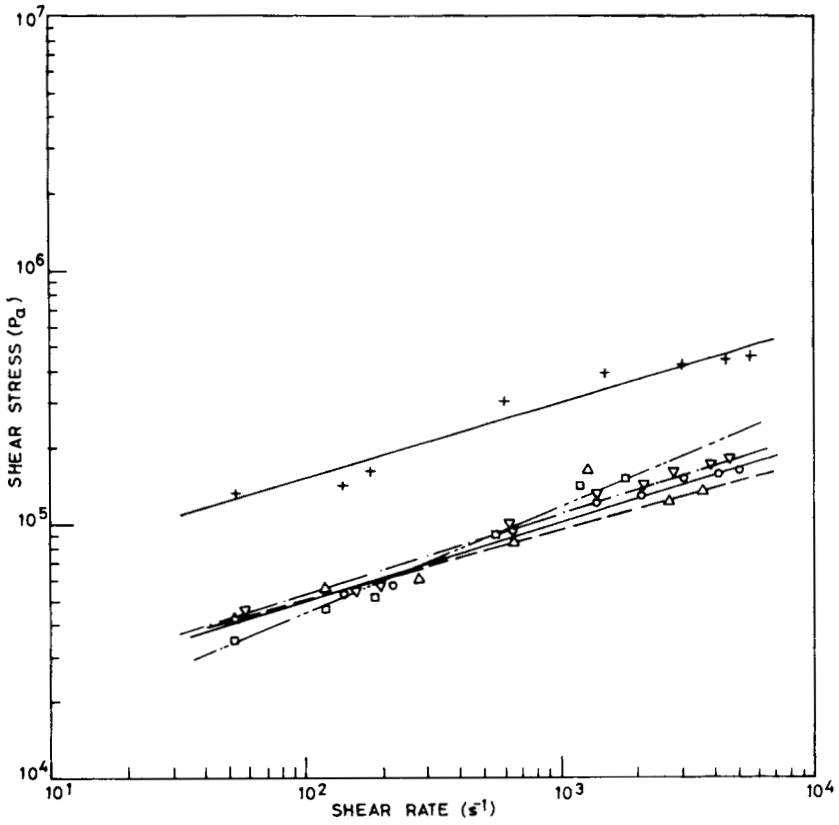

Figure 1 Variation of shear stress with shear rate of PP (○), EPDM (+), and PP/EPDM and at varying EPDM content (wt %): (△) 10; (▽) 20; (□) 30.

shear stress τ was determined after applying the Bagley correction.[21]

Melt viscosity η and first normal stress ($\tau_{11} - \tau_{22}$) were calculated by following expressions[21]:

$$\eta = \tau_w/\dot{\gamma},$$

$$\tau_{11} - \tau_{22} = \Theta\dot{\gamma}^2$$

where Θ is the first normal stress coefficient calculated by the procedure described elsewhere.[22]

Table II Values of Power Law Exponent *n*

Sample	*n*	Sample	*n*
A	0.31	C1	0.26
E	0.30	C2	0.25
B1	0.27	C3	0.20
B2	0.30	C4	0.31
B3	0.41	C5	0.26
P1	0.30	C6	0.23
P2	0.30	C7	0.26
P3	0.28	C8	0.25
—	—	C9	0.24

Recoverable shear strain γ_R was calculated from the first normal stress difference by using the relationship[21]

$$\gamma_R = (\tau_{11} - \tau_{22})/2\tau_w$$

RESULTS AND DISCUSSION

Flow Curves

PP/EPDM Blend

Flow curves, τ_w versus $\dot{\gamma}$, for PP, EPDM, and their blend at various blending ratios are shown in Figure 1. All these curves are quite linear over the entire range of the data. The flow curve of EPDM is distinctly higher than that of PP, whereas the flow curves of the blend samples are quite in the vicinity of that of PP. Separation between the flow curves for the blend samples increases at higher shear rates.

These linear variations are consistent with the following power law:

$$\tau_w = K\dot{\gamma}^n$$

with K and n related to the intercept and slope of the flow curve. Values of n, the pseudoplasticity in-

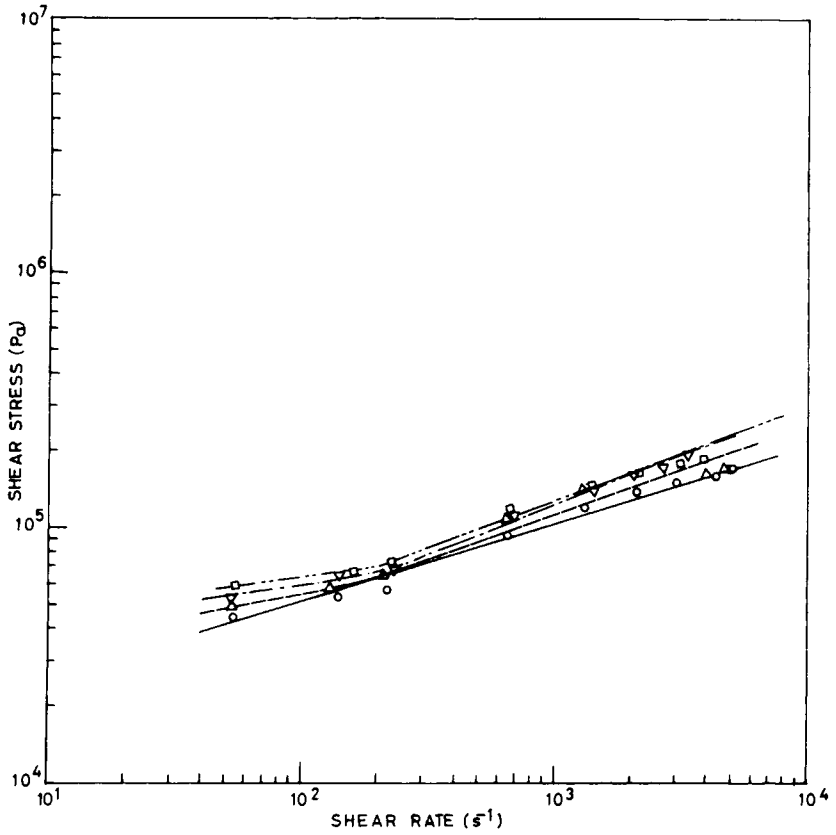

Figure 2 Variation of shear stress with shear rate for PP/GF composite at varying GF content (wt %): (○) 0; (△) 10; (▽) 20; (□) 30.

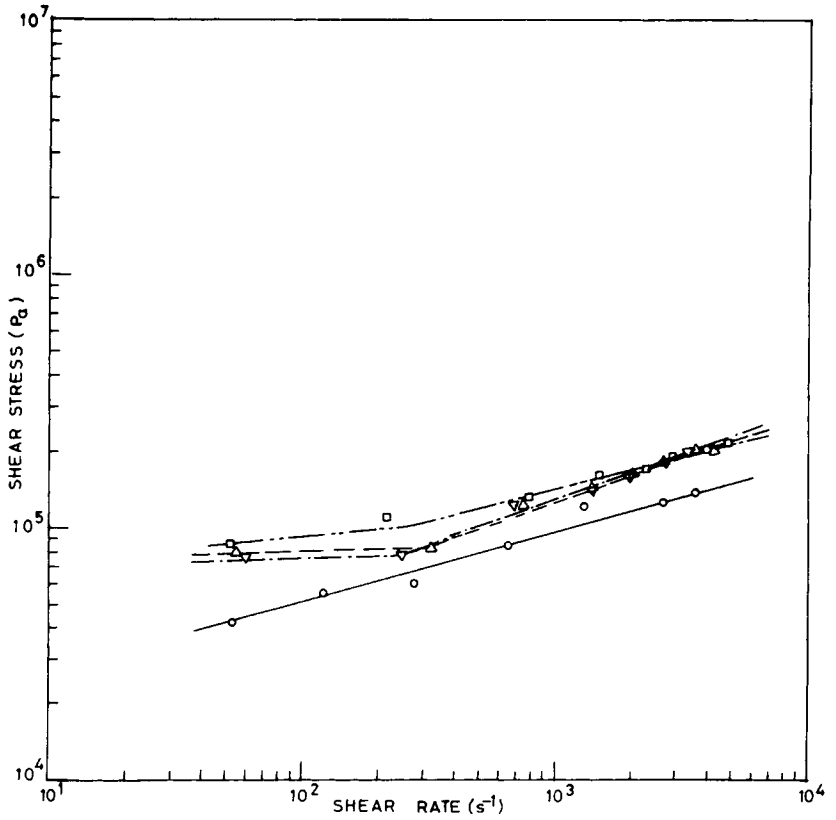

Figure 3 Variation of shear stress with shear rate for PP/EPDM/GF composite at a constant blending ratio (90/10 PP/EPDM) of the matrix and varying GF content (wt %): (○) 0; (△) 10; (▽) 20; (□) 30.

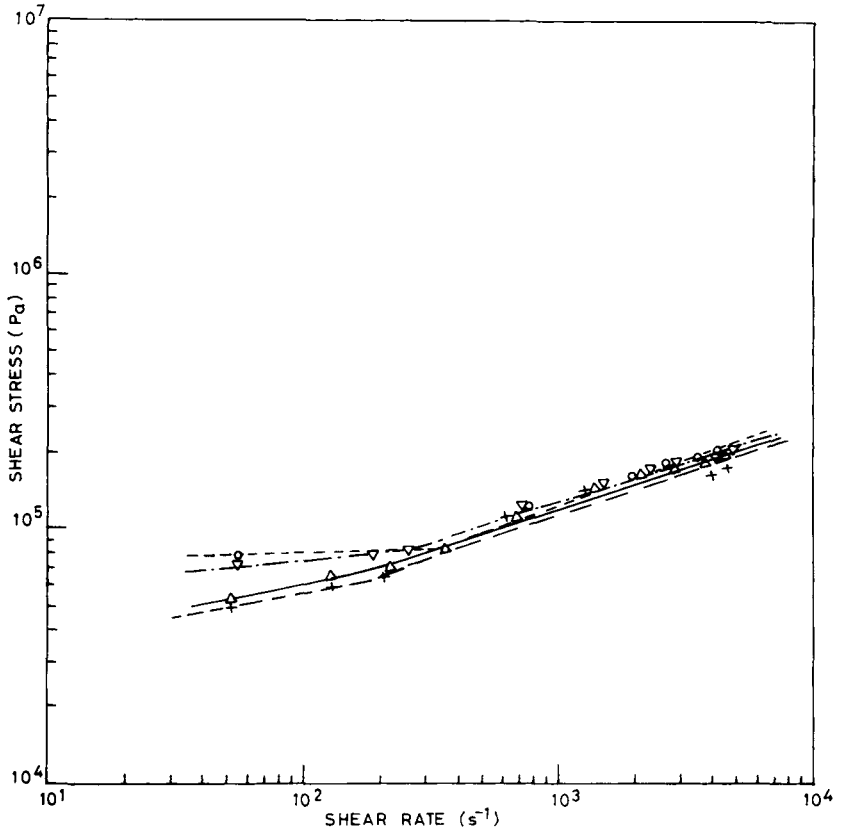

Figure 4 Variation of shear stress with shear rate for PP/EPDM/GF composite at a constant GF loading (10 wt %) and varying blending ratio (PP/EPDM) of the matrix: (+) 100/0; (○) 90/10; (△) 80/20; (▽) 70/30.

dex, shown in Table II, are about 0.3 for both PP and EPDM. Addition of EPDM initially lowers the value of n to 0.27 for 10 wt % EPDM and then increases it with increasing EPDM content up to a value of 0.41 at 30 wt % EPDM content. The significantly different pseudoplasticity of the blend than its individual components, and a systematic variation of the pseudoplasticity index with the blending ratio, implies a significant role of EPDM in the pseudoplasticity of the blend.

PP/EPDM/GF Composite

Two sets of flow curves, τ_w versus $\dot{\gamma}$, for PP/EPDM/GF composite and one for PP/GF composite are presented in Figures 2, 3, and 4 to represent (i) the effect of glass fiber loading in unblended PP matrix (Fig. 2) and at constant blending ratio of the PP/EPDM matrix (Fig. 3) and (ii) the effect of variation of matrix blending ratio at constant glass fiber loading (Fig. 4). A change of slope representing two distinct linear portions is seen for the flow curves for all the samples containing GF, with the change of slope around a critical shear rate $\dot{\gamma}_c = 3 \times 10^2\ s^{-1}$. Higher slope above the critical shear rate implies a higher value of n in the presence of GF. This change of pseudoplasticity of the melt in presence of GF at a critical shear rate indicates an active role of kinetic energy of GF in influencing the flow behaviors of the two components of the matrix (i.e., PP and EPDM).

At shear rates higher than $\dot{\gamma}_c$, the flow curves for samples containing GF (Figs. 2–4) show a tendency of coinciding with each other, implying that the variation of GF content has little effect on the flow at high shear rates. It may be recalled that the variation of EPDM content in the absence of GF produced greater separation of flow curves at higher shear rates (see Fig. 1). At high shear, the role of GF becomes prominent enough to overshadow the effect of variation of EPDM content, hence the separation of flow curves as a function of EPDM content observed in the absence of GF (Fig. 1) is not seen in the presence of GF (Fig. 4). This is further supported by the overlapping of the flow curves in the case of PP/GF at higher shear rates (Fig. 2).

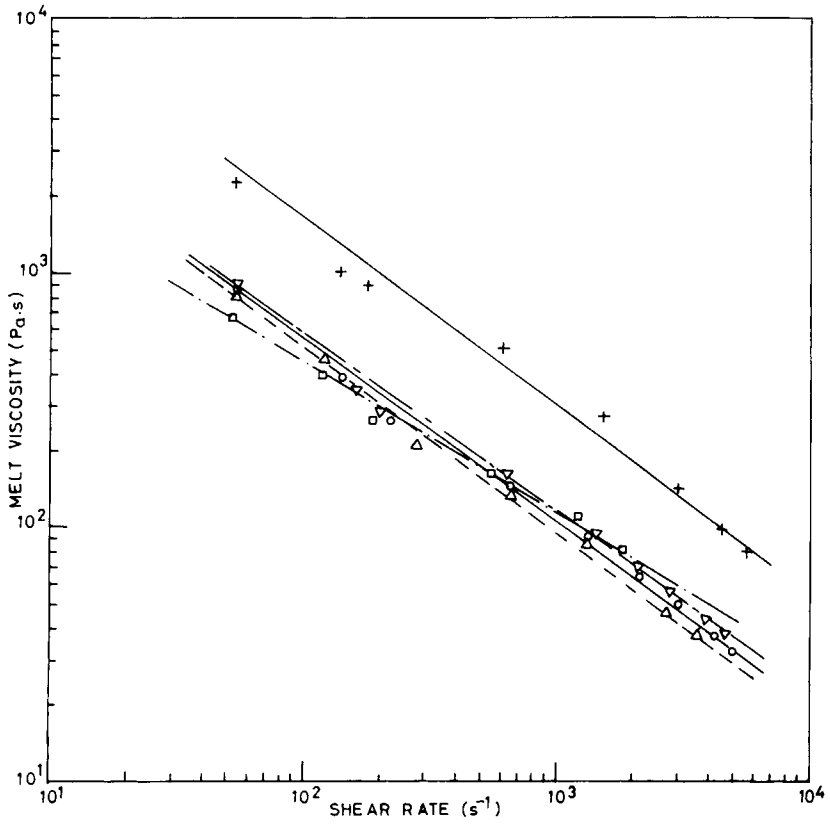

Figure 5 Melt viscosity as a function of shear rate for PP (○), EPDM (+), and PP/EPDM blend at varying EPDM content (wt %): (△) 10; (▽) 20; (□) 30.

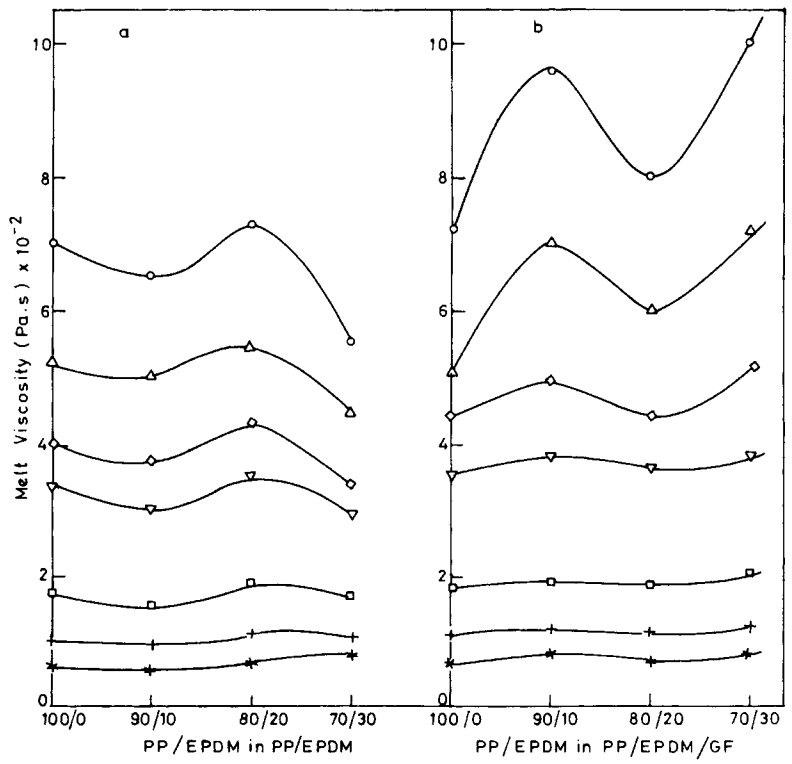

Figure 6 Melt viscosity as a function of blending ratio (PP/EPDM) of the matrix at 0% (a) and 10% (b) GF loading with shear rate (s^{-1}) as the variable: (○) 7×10^1; (△) 1×10^2; (◇) 1.5×10^2; (▽) 2×10^2; (□) 5×10^2; (+) 1×10^3; (*) 2×10^3.

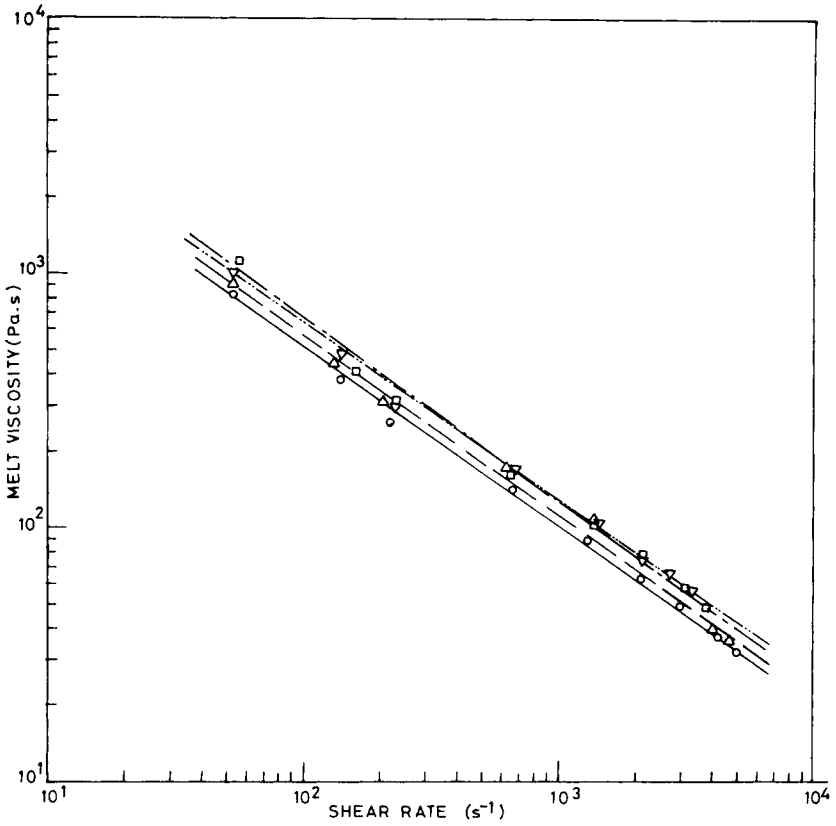

Figure 7 Melt viscosity as a function of shear rate for PP/GF composite at varying GF loading (wt %): (○) 0; (△) 10; (▽) 20; (□) 30.

Flow curves of PP/EPDM (90/10) blend, which is situated below that of PP (see Fig. 1), moves considerably above the flow curve of PP on addition of GF to this blend (see Fig. 3). This implies a significant role of GF in the increase of viscosity of the melt.

Values of the power law exponent n for PP/EPDM/GF composite calculated from the slopes of the flow curves in the region above the critical shear rate are shown in Table II. On addition of GF there is a general decrease of n in comparison to the corresponding matrix (i.e., PP or the PP/EPDM binary blend). The value of n further decreases with increasing GF content for each of the matrix com positions used. This clearly suggests that GF increases the pseudoplasticity of the melt for not only PP but also PP/EPDM blend.

Melt Viscosity

PP/EPDM Blend

Melt viscosity η as a function of shear rate $\dot{\gamma}$ is shown in Figure 5 for PP, EPDM, and PP/EPDM blend. The plots are quite linear for all the samples.

As a function of blend composition, the melt viscosity, at identical shear rates, varies as shown in Figure 6(a). On initial addition of 10 wt % EPDM the melt viscosity decreases slightly and then increases up to its maximum value at 20 wt % EPDM. Thereafter it decreases rather rapidly from 20 to 30 wt % EPDM content. The sharpness of maximum at 20 wt % EPDM decreases with increasing shear rate. Such a variation of sharpness of maxima and minima with shear rate (or shear stress), reported for two-phase blends by other authors, has been attributed[23,24] to the effect of size and size distribution of the dispersed phase domains and the interaction among the dispersed phase domains.

PP/EPDM/GF Composite

Variations of melt viscosity with shear rate for the composite samples are shown in Figures 7–9 for the cases of (i) varying GF content in unblended PP (Fig. 7), (ii) varying GF content at constant blending ratio of the matrix (Fig. 8) and (iii) varying blending ratio of the matrix at constant GF loading (Fig. 9). Also included in these plots are the data

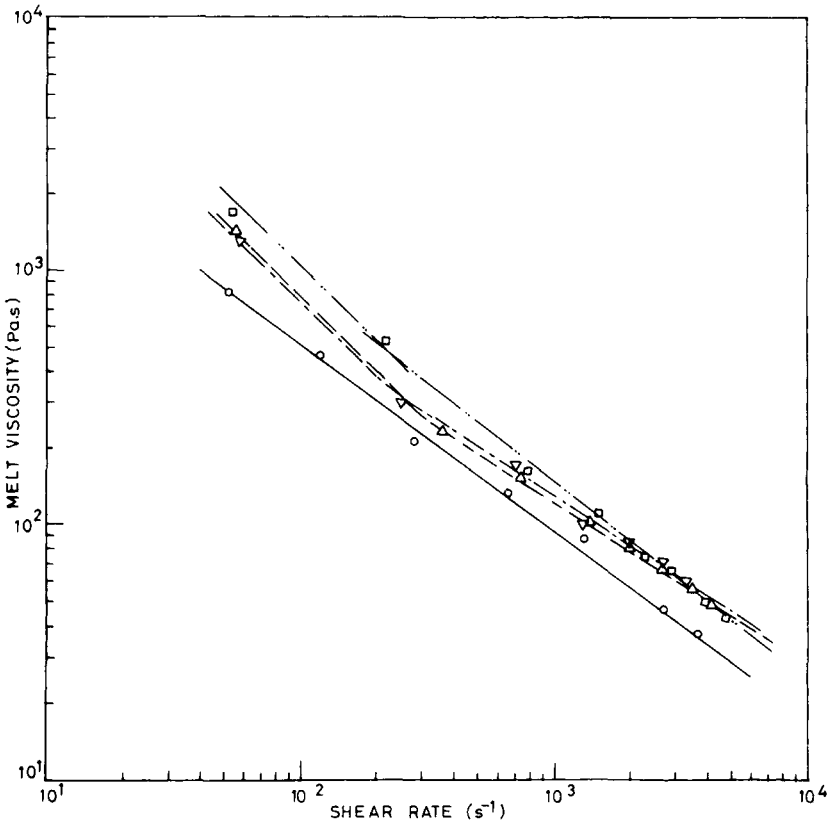

Figure 8 Melt viscosity as a function of shear rate for PP/EPDM/GF composite at constant blending ratio (PP/EPDM 90/10) of the matrix and varying GF loading (wt %): (○) 0; (△) 10; (▽) 20; (□) 30.

for the corresponding reference sample, viz., the matrix in the first two cases (Figs. 7 and 8) and PP/GF 90/10 in the third case (Fig. 9). It is seen that melt viscosity for the composite is higher than that of the corresponding polyblend matrix. Variation of melt viscosity with shear rate in the case of the composites shows two linear portions with change of slope at a shear rate $3 \times 10^2\ s^{-1}$, which is the same as the above-stated critical shear rate. This change of slope is quite significant at small EPDM content and is inappreciable at high EPDM content. As a function of matrix blending ratio, the melt viscosity at fixed shear rates varies as shown in Figure 6(b), which shows maxima and minima at low shear rates and quite flat variation at high shear rates. This suggests that at 90/10 blending ratio the GF produces more obstruction to flow than in case of 80/20 blending ratio, and this effect vanishes with increasing shear rate.

Usually the polymers show an insignificant variation of melt viscosity with shear rate at low shear rates and sharp decrease of melt viscosity with increasing shear rate above shear rates $10^3\ s^{-1}$. However, for these data on PP and PP/EPDM blend, the η versus $\dot{\gamma}$ curves are quite linear over the entire range whereas the data points for EPDM give an impression of continuously changing slope of the curve (not drawn in the figure), indicating a smaller variation at lower shear rates. On the other hand, the GF containing samples show a sharper variation of melt viscosity in the lower shear rate range than at higher shear rates. A change of slope at around $\dot{\gamma} = 3 \times 10^2\ s^{-1}$ is seen in all the GF-containing samples. The upward slope of η versus $\dot{\gamma}$ curve at low shear rates seems attributable to the effect of the GF filler. Similar upward deflection of η versus $\dot{\gamma}$ curve at low shear rates is reported by other authors for polymer melts in the presence of rigid fillers.[2-5,10,14-17] Such a behavior could be attributed to the relative predominance of extensional and shear flow. At low shear rates, extensional flow predominates whereas at high shear rates (i.e., above the critical shear rate) shear flow becomes predominant. Extensional flow produces alignment of glass fibers in flow direction while shear flow aligns the fibers at an angle with the flow direction. Hence the viscosity reduction (i.e., ease of flow due to alignment of glass fibers) is better in the case of extensional flow than shear flow. The observed faster rate of decrease of melt viscosity with increasing shear rate, in the region below the critical shear rate, confirms the predominance of extensional flow below the

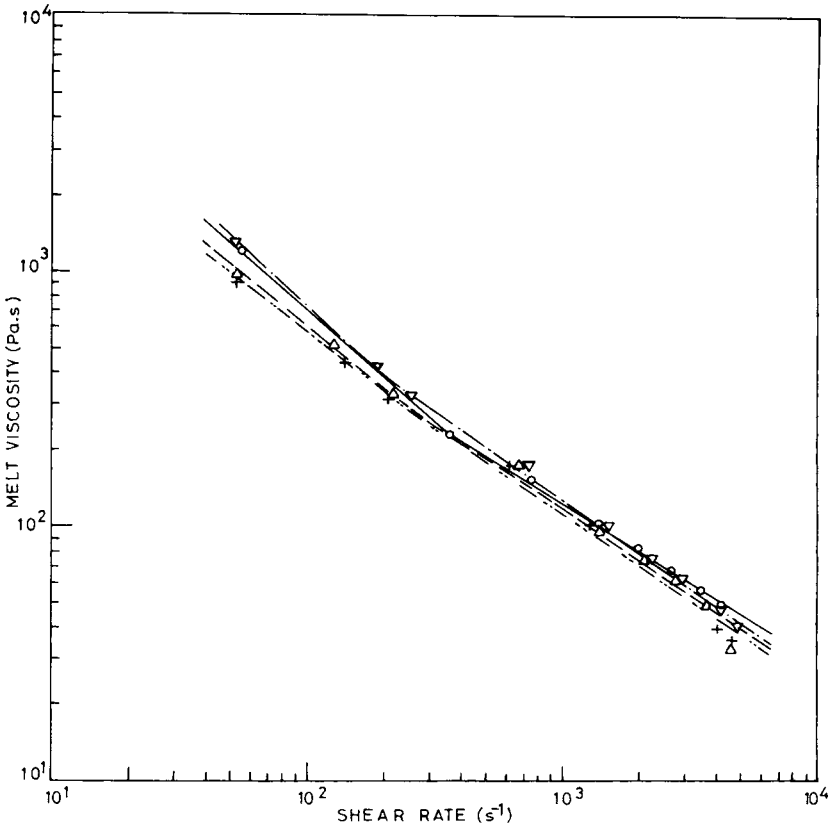

Figure 9 Melt viscosity as a function of shear rate for PP/EPDM/GF composite at constant GF loading (10 wt %) at varying blending ratio (PP/EPDM) of the matrix: (+) 100/0; (○) 90/10; (△) 80/20; (▽) 70/30.

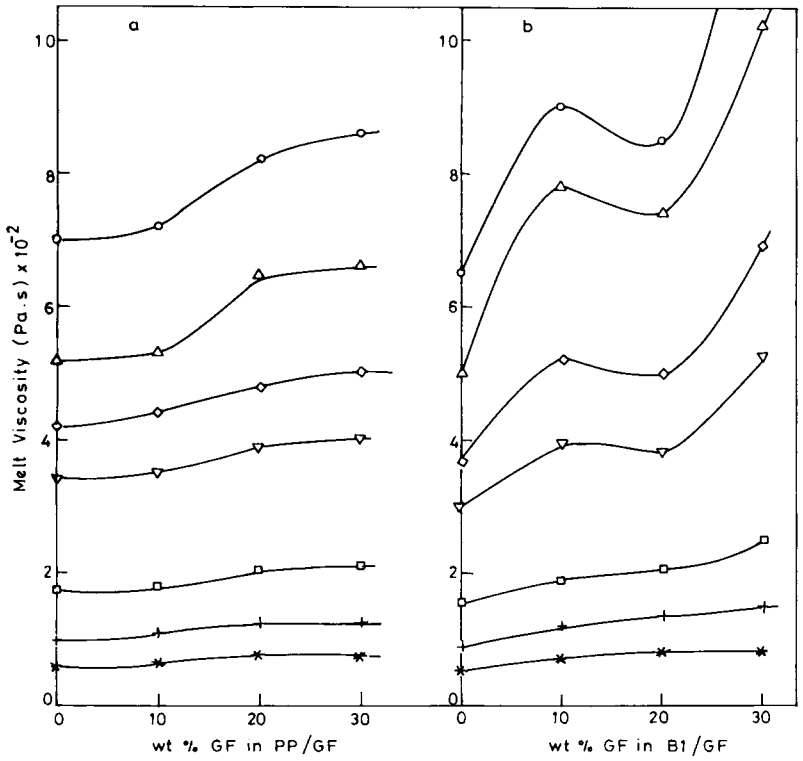

Figure 10 Melt viscosity as a function of GF loading in (a) PP/GF, and (b) PP/EPDM/GF at fixed matrix compositions (PP/EPDM 90/10) with shear rate (s^{-1}) as the variable: (○) 7×10^1; (△) 1×10^2; (◇) 1.5×10^2; (▽) 2×10^2; (□) 5×10^2; (+) 1×10^3; (*) 2×10^3).

critical shear rate. Other authors[25] have also reported that the extensional flow induces greater fiber alignment than shear flow, and produces a reduction of viscosity till the fibers are well oriented in flow direction and thereafter the viscosity change is essentially due to shear flow.

Furthermore, the η versus $\dot{\gamma}$ plots for samples containing GF show a good mutual overlap at high shear rates in all cases. This overlapping tendency is an effect of greater orientation of GF at high shear rates. This is further supported by the observation that at low shear rates the curves are rather well separated and the difference due to GF loading is prominent only at low shear rates. The GF seems to have greater effect than EPDM on the melt flow of the ternary system PP/EPDM/GF particularly at low shear rates where the variation of GF content produces greater variation of the viscosity than the variation of EPDM content (compare Figs. 8 and 9). At any instant during the flow of this three-phase mixture, the fluid of the major component PP carries with it the GF and EPDM domains. The perfectness of the alignment of the GF in the flow direction depends on the shear rate. During their passage, the glass fibers may collide with the EPDM domains and get deflected in random directions. Thus the EPDM domains may cause disturbance in the alignment of the glass fibers with respect to flow direction, which, in turn, may increase the obstruction to flow or the melt viscosity. The degree of this obstruction to flow depends not only on the interaction of the GF and the EPDM domains, but also on the shear rates. At high shear rates, the randomization of the GF alignment will be further reduced by the shearing force of the matrix fluid. Therefore, the effect of GF on melt viscosity may be expected to be less at higher shear stress (or higher shear rates). In the region of low shear rates, the melt viscosity increases with increasing GF content (Fig. 10), which also supports the above explanation.

Variation of GF content, at a constant blending ratio of the polyblend matrix, produces quite a nonlinear variation of melt viscosity, as shown in Figure 10(b). Initially up to 10% GF content, the melt viscosity rises sharply and then shows a slight decrease up to 20% GF content followed by another sharp

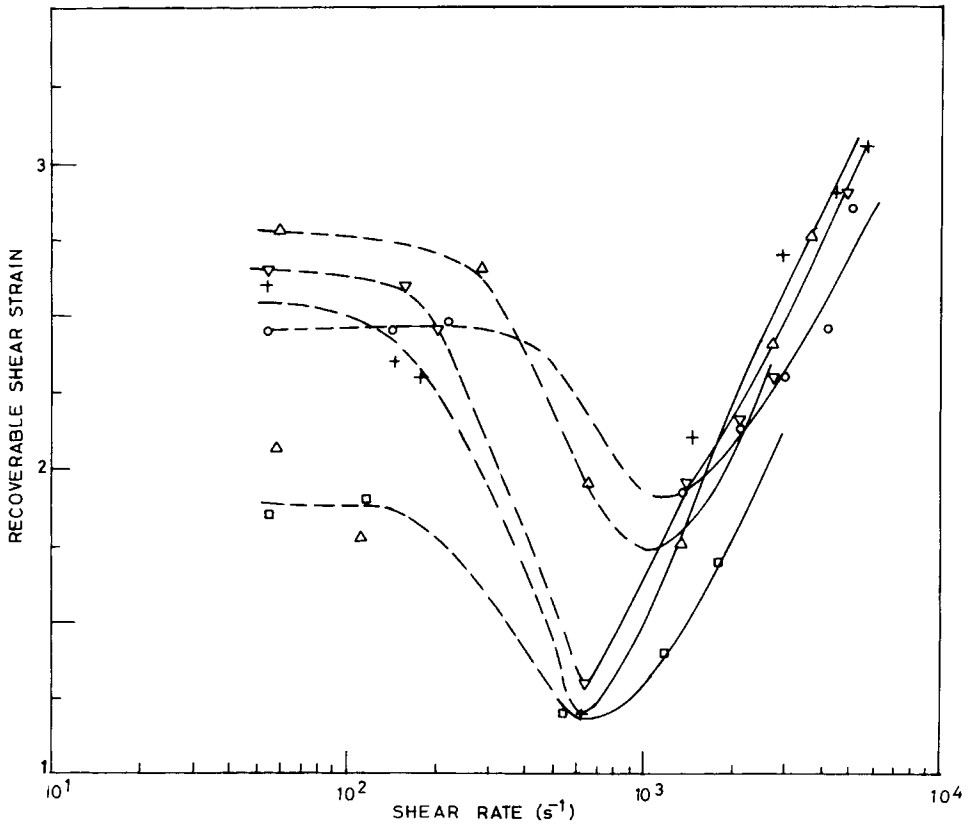

Figure 11 Variation of recoverable shear strain with shear rate for PP/EPDM blend at varying compositions (EPDM wt %): (○) 0; (△) 10; (▽) 20; (□) 30; (+) 100.

increase at higher GF content. The sharpness of the maxima and minima, observed at 10 and 20% GF contents, respectively, decreases with increasing shear rate. This indicates that at high shear rates the randomization of glass fiber alignment on collision with EPDM droplets is reduced owing to the high shearing forces of the flowing fluid. This explains the observed decrease in the dependence of melt viscosity on GF content with increasing shear rate. Crowson et al.,[12,13] for PP/GF and nylon-66/GF systems, have also reported that flow properties become less sensitive to the role of GF at high shear rates.

The overall increase (in the entire range of measurements, i.e., 0–30% GF content) of melt viscosity with increasing GF content, which is observed for rigid solid suspensions by other authors[2-4,10] (and is quite large at low shear rates), is understandable due to the hindrance to flow produced by GF (which are rather randomly aligned at low shear rates). However, the observed small decrease in the region 10–20% GF loading might be due to interaction of dispersed EPDM droplets and GF, as this was not observed in our data on PP/GF [Fig. 10(a)].

Finally, some variations for which figures are not shown are as follows. As a function of EPDM content of the polyblend matrix, at constant GF content, the melt viscosity shows the following behavior: (i) at 10% GF content, the melt viscosity showed a minimum at 80/20 PP/EPDM blending ratio of the matrix; (ii) at 20% GF content, the melt viscosity increased continuously with increasing EPDM content of the matrix; and (iii) at 30% GF content melt-viscosity showed a maximum at 80/20 PP/EPDM blending ratio of the matrix. The sharpness of the maxima and minima decreased with increase in shear rate. This supports the above-stated possibility of the role of interaction of EPDM and GF in the melt flow behavior of this composite.

Melt Elasticity

PP/EPDM Blend

Among the parameters related to the elasticity of the polymer melt, the recoverable shear strain (S_R) is considered the most appropriate for describing elastic behavior of multiphase fluids. Variation of

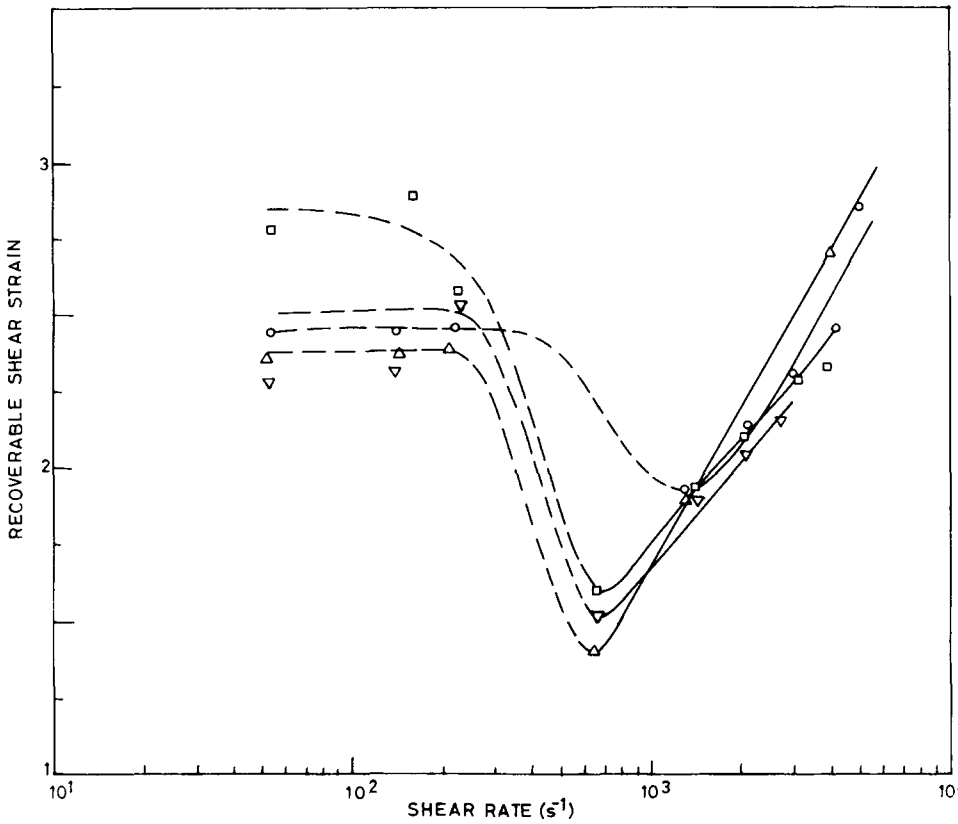

Figure 12 Variation of recoverable shear strain with shear rate for PP/GF composite at varying GF content (GF wt %): (○) 0; (△) 10; (▽) 20; (□) 30.

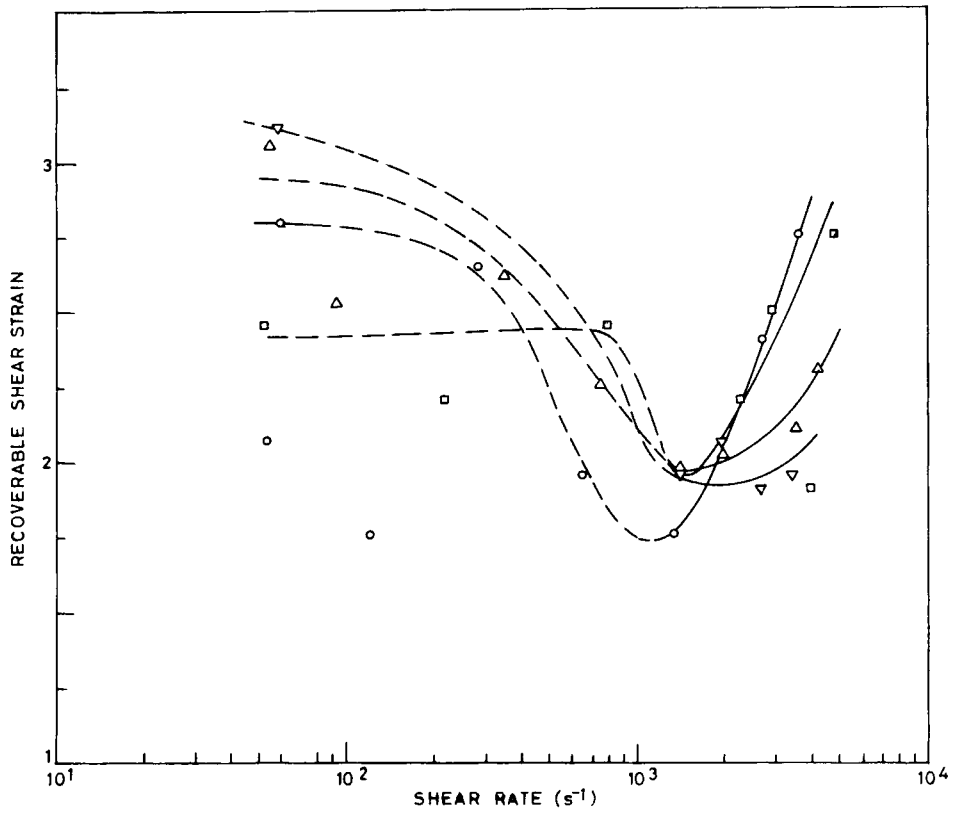

Figure 13 Variation of recoverable shear strain with shear rate for PP/EPDM/GF composite at a blending ratio (90/10 PP/EPDM) of the matrix and varying GF content (wt %): (○) 0; (△) 10; (▽) 20; (□) 30.

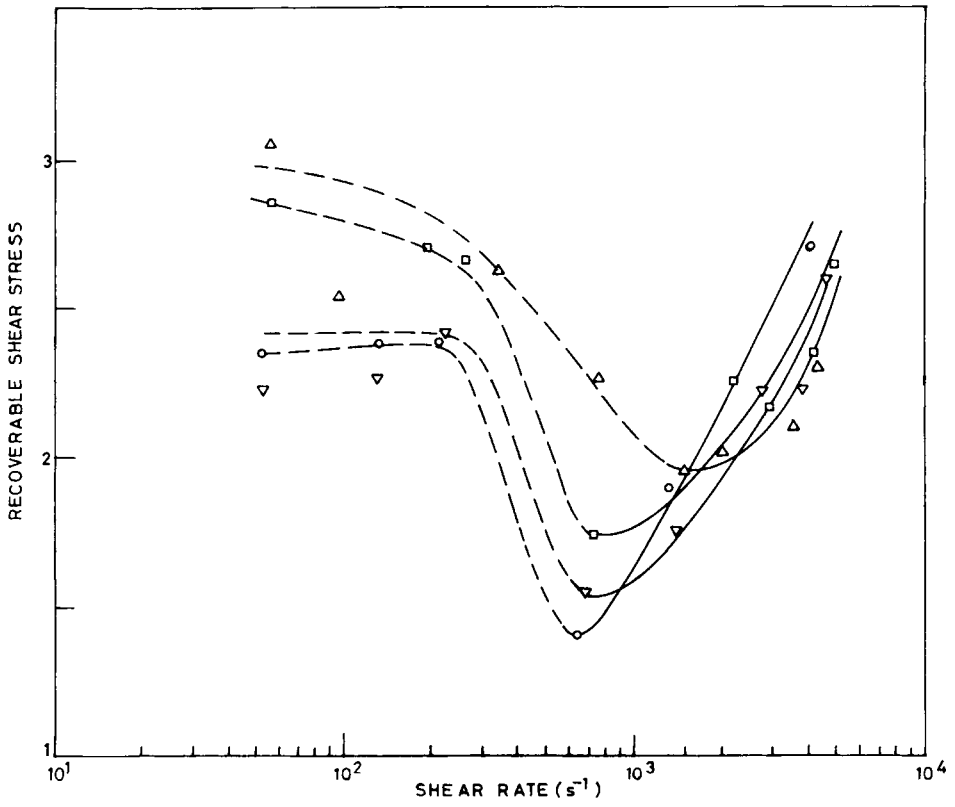

Figure 14 Variation of recoverable shear strain with shear rate for PP/EPDM/GF composite at constant GF loading (10 wt %) and varying blending ratio (PP/EPDM) of the matrix: (○) 100/0; (△) 90/10; (▽) 80/20; (□) 70/30.

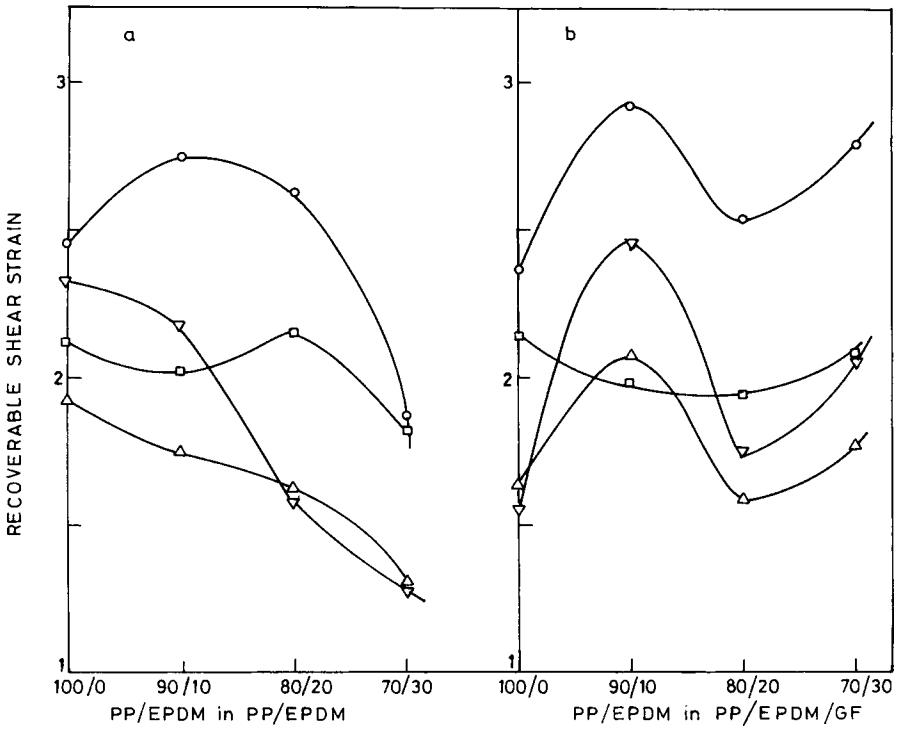

Figure 15 Recoverable shear strain as a function of blending ratio (PP/EPDM) of the matrix at (a) 0% and (b) 10% GF loading with shear rate (s^{-1}) as the variable: (○) 1×10^2; (▽) 5×10^2; (△) 1×10^3; (□) 2×10^3.

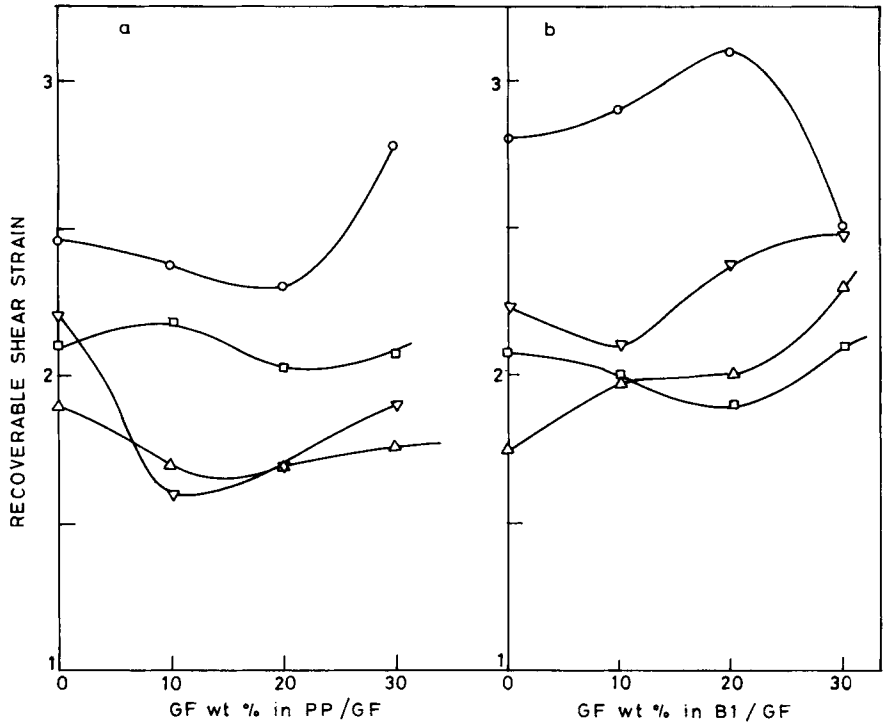

Figure 16 Recoverable shear strain as a function GF loading in (a) PP/GF and (b) PP/EPDM/GF at fixed matrix composition (PP/EPDM 90/10) with shear rate (s^{-1}) as the variable: (○) 1×10^2; (▽) 5×10^2; (△) 1×10^3; (□) 2×10^3.

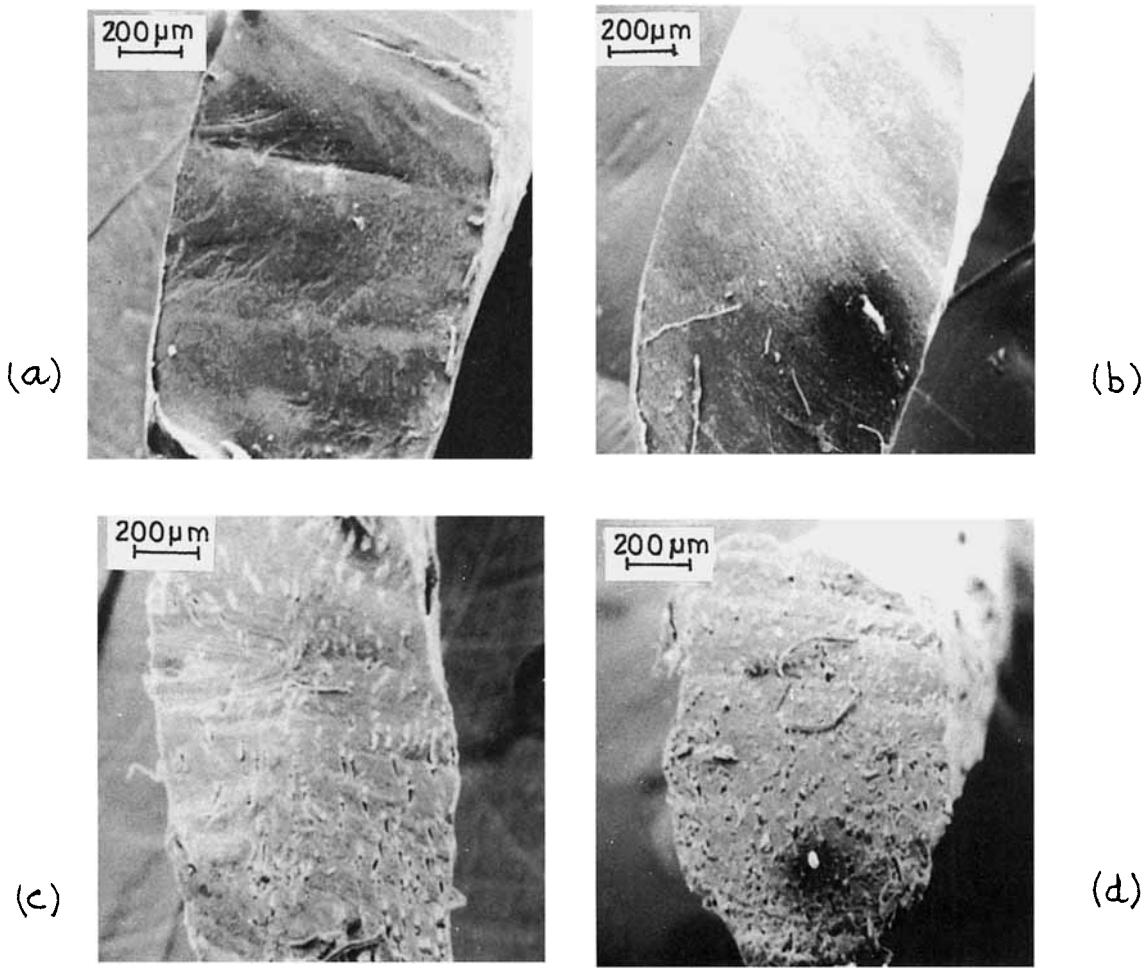

Figure 17 Scanning electron micrographs of rheometer extrudates of (a) PP, (b) PP/EPDM (90/10), (c) B2/GF (80/20), and (d) B2/GF (70/30).

S_R with shear rate for PP, EPDM, and PP/EPDM blend are shown in Figure 11. At shear rates above 10^3 s^{-1} the S_R increases sharply with increasing shear rate for all the samples. However, at lower shear rates (i.e., $\dot{\gamma} < 10^3$ s^{-1}) the scatter of data points is large and the approximate trends of variation discerned from these data are shown by broken curves. In the range of low shear rate S_R remains constant up to the shear rate 2×10^2 s^{-1} and then decreases sharply with increasing shear rate up to its minimum value at shear rate slightly less than 10^3 s^{-1}. This behavior at low shear rates is quite strange and seems to arise due to nonequilibrium state of elastic recovery.

PP/EPDM/GF Composite

For the case of glass fiber in the PP matrix, the variation of S_R with shear rate, shown in Figure 12, has the same features as seen for PP/EPDM blend in Figure 11. Melt elasticity of PP/GF and PP/EPDM systems increases with shear rate at $\dot{\gamma} > 10^3$ s^{-1} quite similarly as may be seen from equal slopes of the curves in Figures 11 and 12.

The effect of GF in PP/EPDM matrix is represented in Figures 13 and 14 at constant EPDM and varying GF loading in the former case and constant GF and varying EPDM loading in the latter. The scatter of data in these three component systems is greater than that in the previous cases of two component systems (Figs. 11 and 12). This indicates that the displacement from equilibrium is greater in the three-component system than the two-component system. The scatter of data points even at high shear rates in these three-component systems indicates greater possibility of nonequilibrium effects in the three-component systems. The interaction of GF with the dispersed EPDM droplets is responsible for nonequilibrium effects in elastic recovery. Nor-

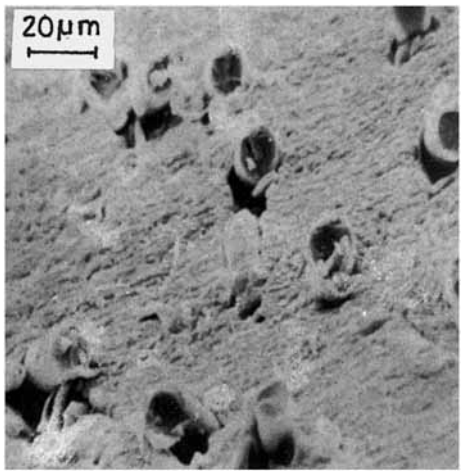

(a)

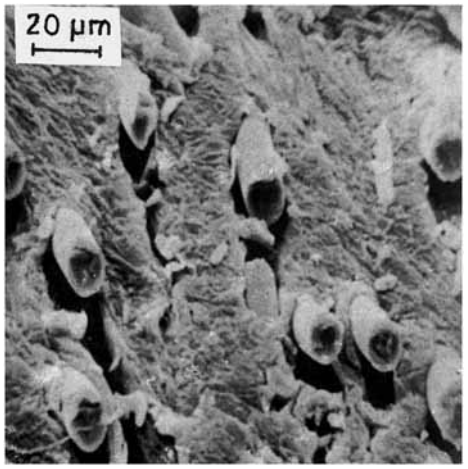

(b)

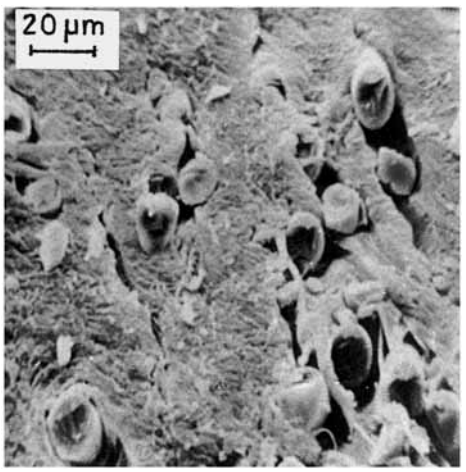

(c)

Figure 18 Scanning electron micrographs of rheometer extrudates of (a) B2/GF (90/10), (b) B2/GF (80/20), and (c) B2/GF (70/30).

mally at high shear rates, such effect should minimize, owing to greater possibility of alignment of the dispersed components in the flow direction. Furthermore, for the case of increasing GF content at a constant blending ratio of the polyblend matrix, the nonequilibrium effects in elastic recovery increase, and produce greater scatter of data points at high shear rates, as seen in Figure 13. However, at constant GF loading the nonequilibrium effects show quite inappreciable variation with the blending ratio of the polyblend matrix, as seen from the small scatter of data around the linear extrapolations at high shear rates in Figure 14. This suggests that GF obstructs the elastic recovery of the melt more than the dispersed elastomer domains. This effect of GF is more distinct in the presence of the EPDM droplets in PP matrix than in PP matrix alone.

As a function of blending ratio of PP/EPDM, S_R shows an overall decrease with increasing EPDM content without any sharp maxima or minima [Fig. 15(a)]. The decrease of melt elasticity on incorporation of elastomers is a general feature of polymers, also observed on PP/SEBS[18] and PP/ABS[20] blends, and is attributed to lesser elastic recovery of the elastomer droplets. On the other hand, the variation of S_R with PP/EPDM ratio in PP/EPDM/GF composite at constant GF content (10 wt %) [Fig. 15(b)] suggests an overall slight increase with a sharp maximum around 90/10 PP/EPDM blending ratio except at the highest shear rate. Thus the results shown in Figures 15(a) and (b) clearly distinguish between the roles of GF and EPDM droplets in the elasticity of the melt.

Variation of S_R with GF content in PP and the blend B1 (i.e., PP/EPDM 90/10), shown in Figure 16, is quite small at high shear rates. However, at low shear rates the distinction is quite clear at high GF content, i.e., 20–30%; for PP/GF S_R sharply increases while for B1/GF it decreases sharply. This supports the presence of the interaction of GF and EPDM and its effect on the melt elasticity of the PP/EPDM/GF ternary system. This effect gradually disappears with increasing shear rate.

Scanning Electron Microscopy

Scanning electron micrographs of cross sections of the rheometer extrudates are presented in Figure 17 for PP, PP/EPDM binary blend, and PP/EPDM/GF composite at two GF loadings. Features of knife shear lines are visible in these micrographs of microtomed specimens. EPDM domains are not distinguishable in these micrographs probably due to the low magnification and/or their indistinguishability with PP. In case of the composites GF are

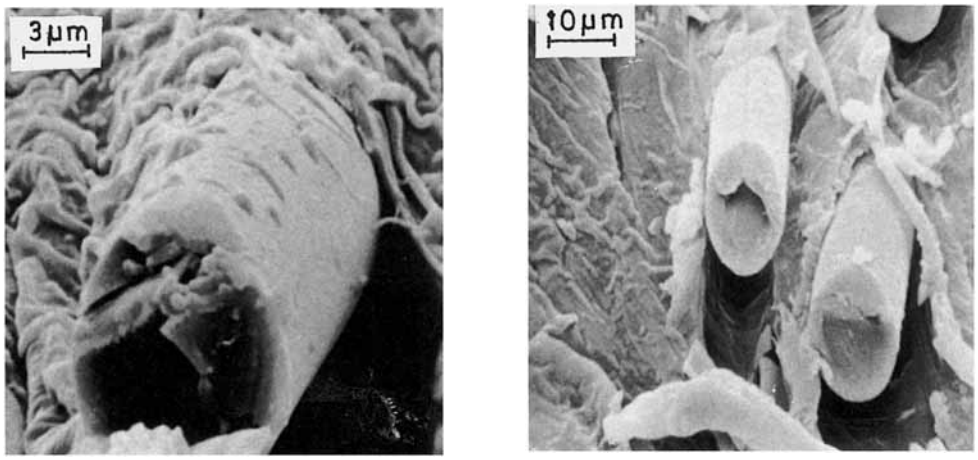

Figure 19 Scanning electron micrographs of rheometer extrudates of (a) B2/GF (90/10) and (b) B2/GF (70/30).

clearly visible in the micrographs, and are quite uniformly dispersed [Figs. 17(c) and (d)].

Micrographs of extrudate cross sections at higher magnifications (Fig. 18) show that the GF are perpendicular to the cross-sectional surface, or in other words, the glass fibers are aligned along the flow direction, i.e., the axis of the extrudate.

The glass fibers are apparently closely held by the matrix, except that there are some gaps between the matrix and the fiber created due to the shearing force of the knife. These gaps are invariably on one and the same side of the GF, which confirms that they are not due to differential contraction of the GF and the surrounding matrix. Micrographs at still higher magnifications, shown in Figure 19, present a more clear view of the gaps created between the glass fiber and the matrix. The surface of GF at such high magnification [Fig. 19(a)] shows some traces of polymer sticking on it. This might be the EPDM component of the matrix. The fact that effect of EPDM remains on the GF surface after the fracture indicates that EPDM has a better bonding tendency with GF than PP.

CONCLUSION

Flow curves of PP/EPDM blend are quite linear in measured shear rate range 10^1–10^4 s^{-1}, with power law exponent (n) increasing from about 0.3 to 0.4, with increasing EPDM content. Addition of GF lowers down the value of n in both PP and PP/EPDM blend and the flow curve undergoes a change of slope around a shear rate of 3×10^2 s^{-1}.

At high shear, the glass fibers are well aligned and hence the variation of the viscosity with fiber concentration becomes inappreciable. However, in the absence of GF the viscosity variation with EPDM concentration is quite significant at high shear rates.

Melt viscosity shows overall increase with increasing GF content in both PP and PP/EPDM blend, with a little nonlinearity in the middle of the range, which seems to be due to the interaction of the EPDM droplets and the glass fibers.

Melt elasticity of PP and PP/EPDM blend decreases only up to 20 wt % GF loading. At higher GF loading the melt elasticity increases, which is apparently a combined shear dependent effect of GF and dispersed elastomer droplets. Variation of melt elasticity with shear rate is nonlinear with considerable scatter of data points and shows an increase of melt elasticity with shear rate only above a shear rate about 10^3 s^{-1}. The nonlinear variation of melt elasticity with shear rate is attributed to nonequilibrium of elastic recovery in the presence of GF and these effects are further enhanced in the presence of the elastomer domains, which is attributed to randomization of GF orientation on collision with EPDM droplets.

Scanning electron microscopy of the extrudates shows that (i) the EPDM domains are not distinguishable in PP matrix, (ii) the glass fibers are closely held by the matrix, and (iii) glass fibers are aligned parallel to fracture.

REFERENCES

1. C. D. Han, *Multiphase Flow in Polymer Processing*, Academic, New York, 1981.

2. N. Minagawa and J. L. White, *J. Appl. Polym. Sci.*, **20,** 501 (1976).
3. V. M. Lobe and J. L. White, *Polym. Eng. Sci.*, **19,** 617 (1979).
4. C. D. Han, T. Van den Weghe, P. Shete, and J. R. Haw, *Polym. Eng. Sci.*, **21,** 196 (1981).
5. J. L. White and J. W. Crowder, *J. Appl. Polym. Sci.*, **18,** 1013 (1974).
6. J. M. Charrier and J. M. Rieger, *Fibre Sci. Technol.*, **7,** 161 (1974).
7. Y. Chan, J. L. White, and Y. Oyanaga, *J. Rheol.*, **22,** 507 (1978).
8. H. Tanaka and J. L. White, *Polym. Eng. Sci.*, **2,** 949 (1980).
9. L. Czarnecki and J. L. White, *J. Appl. Polym. Sci.*, **25,** 1217 (1980).
10. F. M. Chapman and T. S. Lee, *SPE J.*, **26,** 37 (1970).
11. D. McNally, *Polym. Plast. Technol. Eng.*, **8,** 101 (1977).
12. R. J. Crowson, M. J. Folkes, and P. F. Bright, *Polym. Eng. Sci.*, **20,** 925 (1980).
13. R. J. Crowson and M. J. Folkes, *Polym. Eng. Sci.*, **20,** 934 (1980).
14. J. E. Stamhuis and J. P. A. Loppe, *Rheol. Acta*, **21,** 103 (1982).
15. T. Kitano, T. Kataoka, T. Nishimura, and T. Sakai, *Rheol. Acta*, **19,** 764 (1980).
16. T. Kataoka, T. Kitano, Y. Oyanagi, and M. Sasahara, *Rheol. Acta*, **18,** 635 (1979).
17. T. Kataoka, T. Kitano, M. Sasahara, and K. Nishijima, *Rheol. Acta*, **17,** 149 (1978).
18. A. K. Gupta and S. N. Purwar, *J. Appl. Polym. Sci.*, **29,** 1079 (1984).
19. A. K. Gupta and S. N. Purwar, *J. Appl. Polym. Sci.*, **30,** 1777 (1985).
20. A. K. Gupta, A. K. Jain, and S. N. Maiti, *J. Appl. Polym. Sci.*, **38,** 1699 (1989).
21. C. D. Han, *Rheology in Polymer Processing*, Academic, New York, 1976, Chap. 5.
22. W. Gleissle, *Rheol. Acta*, **21,** 485 (1982).
23. C. D. Han, Y. W. Kin, and S. J. Chen, *J. Appl. Polym. Sci.*, **19,** 283 (1975).
24. Reference 1, Chap. 7.
25. G. F. Modlen, *J. Mater. Sci.*, **4,** 283 (1969).
26. Reference 1, Chap. 4.

Received April 30, 1990
Accepted Augsut 31, 1990